Reset control performance improvement using fractional derivatives

Valério, Duarte; Saikumar, Niranjan; Dastjerdi, Ali Ahmadi; Karbasizadeh, Nima; Hosseinnia, S. Hassan

DOI
10.1016/j.ifacol.2024.08.197

Publication date
2024

Document Version
Final published version

Published in
IFAC-PapersOnline

Available online at www.sciencedirect.com

ScienceDirect

IFAC PapersOnline CONFERENCE PAPER ARCHIVE

IFAC PapersOnLine 58-12 (2024) 243–248

Reset control performance improvement using fractional derivatives ⋆

Duarte Valério * **Niranjan Saikumar** **
Ali Ahmadi Dastjerdi ** **Nima Karbasizadeh** ***
S. Hassan HosseinNia ****

* *IDMEC, Instituto Superior Técnico, Universidade de Lisboa, Lisboa, Portugal (e-mail: duarte.valerio@tecnico.ulisboa.pt).*
** *Nearfield Instruments, Rotterdam*
*** *ASML, Veldhoven*
**** *Department of Precision and Microsystems Engineering, Delft University of Technology, Delft, The Netherlands (e-mail: S.H.HosseinNiaKani@tudelft.nl)*

Abstract: When a linear controller is replaced by a reset controller, it is possible to keep the gain behaviour essentially the same, while improving the phase behaviour. However, because reset control is nonlinear, higher order harmonics appear, which may deteriorate the results. In this paper, reset controllers are combined with fractional derivatives, decreasing the magnitude of higher order harmonics. In this way, better results are found in simulations of a Clegg integrator, of a FORE (first order reset element), and of a CgLp (constant in gain lead in phase) controller. The reason why better results are found is explained.

Keywords: Discontinuous control; Fractional-order systems; Reset control; Clegg integrator; Describing function.

1. INTRODUCTION

Among non-linear control techniques, reset control is one of the simplest. In its original form, controller states are set to zero (i.e. reset) when the input of the controller is zero. In a generalised form, states undergo a discontinuity, which does not need to be a full reset to zero, when the input is zero. Reset controllers are particular cases of impulsive control systems (Yang et al., 2019).

While replacing a linear controller with a reset controller can improve the performance (Chen et al., 2020), this is not without a cost. As for non-linear controllers in general, stability conditions are harder to establish, and steady-state responses more difficult to find. Frequency responses do not exist, since the steady-state output of a non-linear plant with a sinusoidal input is not linear. However, as long as the output is periodic, it is possible to find an approximate frequency response, called describing function, that approximates the output by the first harmonic of its Fourier series expansion. For better accuracy, this describing function should be complemented with the higher harmonics as well, which can affect stability or at least deteriorate control performance (Saikumar et al., 2021, 2023; Nuij et al., 2006).

After presenting some generalities on reset controllers (section 2), this paper shows that three reset controllers of increasing complexity have their higher harmonics reduced at certain frequencies by combining them with fractional order derivatives. It is then a simple design problem to match the frequencies at which higher harmonics are reduced with those where stability or performance problems might arise. The reset controllers addressed are the Clegg integrator (section 3), the first order reset element (FORE, section 4), and the constant in gain lead in phase controller (CgLp, section 5). Controller performance is found numerically. Section 6 explains why these controllers have their frequency behaviour improved in this way.

The control architectures presented in this paper are new; they differ from other ones, also involving reset control and fractional derivatives, where fractional controllers themselves are being reset (Saikumar and HosseinNia, 2017; Chen et al., 2020; Karbasizadeh et al., 2021). The state of the art for the Clegg, FORE and CgLp controllers is summed up at the beginning of the corresponding sections.

2. GENERALITIES ON RESET CONTROLLERS

Consider a dynamic linear system $\hat{G}(s)$ with N states, i.e. with an $N \times N$ state matrix $\mathbf{A}$:

$$\dot{x}(t) = \mathbf{A}x(t) + \mathbf{B}e(t), \qquad \text{if } e(t) \neq 0 \tag{1}$$
$$u(t) = \mathbf{C}x(t) + \mathbf{D}e(t) \tag{2}$$

The controller's input is $e(t)$ and its output is $u(t)$.

When this system is subject to reset, this is denoted by $\hat{G}(s)$, with the arrow indicating reset. State equations become non-linear:

⋆ The authors acknowledge Fundação para a Ciência e a Tecnologia (FCT) for its financial support via the project LAETA Base Funding (DOI: 10.54499/UIDB/50022/2020).

10.1016/j.ifacol.2024.08.197

$$\dot{x}(t) = \mathbf{A}x(t) + \mathbf{B}e(t), \quad \text{if } e(t) \neq 0 \tag{3}$$
$$x(t^+) = \mathbf{A}_\rho x(t), \quad \text{if } e(t) = 0 \tag{4}$$
$$u(t) = \mathbf{C}x(t) + \mathbf{D}e(t) \tag{5}$$
$$\mathbf{A}_\rho = \text{diag}\,(\gamma_1, \ldots, \gamma_N) \tag{6}$$

In these state equations, the γ_n, $n = 1, 2, \ldots N$ are called the reset coefficients; there is one for each state. As mentioned in section 1, when $\gamma_n = 0$ we say that state n undergoes full reset, and when $\gamma_n \neq 0$ that it undergoes partial reset.

It can be shown (Guo et al., 2009) that the describing function $\hat{G}(j\omega)$ is given by

$$\hat{G}(j\omega) = \mathbf{C}(j\omega\mathbf{I} - \mathbf{A})^{-1}(\mathbf{I} + j\mathbf{\Theta}_\gamma(\omega))\mathbf{B} + \mathbf{D} \tag{7}$$
$$\mathbf{\Theta}_\gamma(\omega) = -\frac{2\omega^2}{\pi}\mathbf{\Delta}(\omega)\left[\mathbf{\Gamma}_\gamma(\omega) - \mathbf{\Lambda}^{-1}(\omega)\right] \tag{8}$$
$$\mathbf{\Lambda}(\omega) = \omega^2\mathbf{I} + \mathbf{A}^2 \tag{9}$$
$$\mathbf{\Delta}(\omega) = \mathbf{I} + e^{\frac{\pi}{\omega}\mathbf{A}} \tag{10}$$
$$\mathbf{\Delta}_\gamma(\omega) = \mathbf{I} + \mathbf{A}_\rho e^{\frac{\pi}{\omega}\mathbf{A}} \tag{11}$$
$$\mathbf{\Gamma}_\gamma(\omega) = \mathbf{\Delta}_\gamma^{-1}(\omega)\mathbf{A}_\rho\mathbf{\Delta}(\omega)\mathbf{\Lambda}^{-1}(\omega) \tag{12}$$

and that the higher order harmonics are given by (Saikumar et al., 2021, 2023)

$$\hat{G}^n(j\omega) = \mathbf{C}(nj\omega\mathbf{I} - \mathbf{A})^{-1}j\mathbf{\Theta}_\gamma(\omega)\mathbf{B}, \quad \text{for odd } n \geq 3 \tag{13}$$
$$\hat{G}^n(j\omega) = 0, \quad \text{for even } n \geq 2 \tag{14}$$

where n is the order of the harmonic (for $n = 1$, the harmonic is, of course, given by (7)).

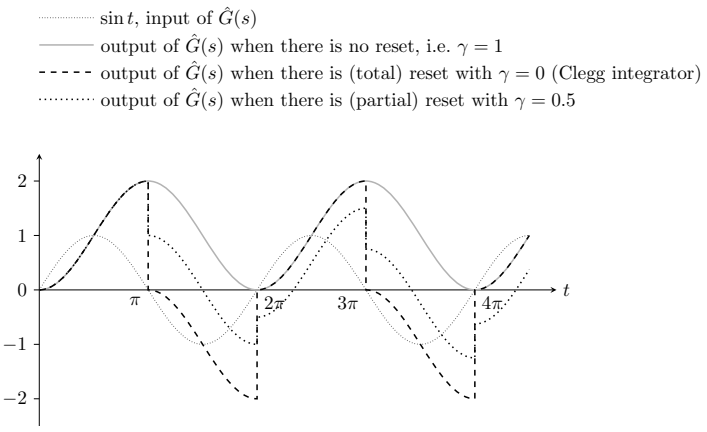

Fig. 1. Response of a reset integrator to a sinusoidal input.

3. CLEGG INTEGRATOR

A Clegg integrator is a variation of an integrator $\frac{1}{s}$, whereby the integral's output is set to zero when the input is zero (Clegg, 1958). To reset the output of a controller, a state-space representation for which the output is one of the states (such as the observable canonical form) is used. A Clegg integrator can be generalised using partial reset. Both situations (the latter for a reset coefficient $\gamma = \frac{1}{2}$) are shown in Figure 1 for a sinusoidal input. The gain slope of $\frac{1}{s}$ is also the gain of the describing function of $\frac{1}{s}$, but the Clegg integrator has a phase closer to zero, which is better for control since phase margins will be wider. Indeed, the state-space representation of the Clegg integrator is

$$\mathbf{A} = 0 \tag{15}$$
$$\mathbf{B} = 1 \tag{16}$$
$$\mathbf{C} = 1 \tag{17}$$
$$\mathbf{D} = 0 \tag{18}$$
$$\mathbf{A}_\rho = \gamma \tag{19}$$

and replacing this in (7)–(12) gives, after simple calculations,

$$\hat{G}(j\omega) = \frac{1}{j\omega}\left(1 - \frac{4j}{\pi}\frac{\gamma - 1}{\gamma + 1}\right) \tag{20}$$

$$20\log_{10}|G(j\omega)| = \underbrace{-20\log_{10}\omega}_{\text{gain slope of } \frac{1}{s}} + 20\log_{10}\sqrt{1 + \left(\frac{4}{\pi}\frac{\gamma - 1}{\gamma + 1}\right)^2} \tag{21}$$

$$\angle\left[G(j\omega)\right] = -90^\circ + \underbrace{\arctan\frac{4(1-\gamma)}{\pi(1+\gamma)}}_{\text{this is} > 0 \text{ if } 0 < \gamma < 1} \tag{22}$$

3.1 Three blocks in series, the second is a Clegg integrator

Figure 2 shows a Clegg integrator sandwiched between two fractional derivatives, i.e. three blocks in series given by

$$G_1(s) = s^{1-\alpha} \tag{23}$$
$$G_2(s) = \frac{1}{s} \tag{24}$$
$$G_3(s) = s^{\alpha-1} \tag{25}$$

so that the reset of the Clegg integrator $G_2(s)$ depends on the input of the first block $G_1(s)$. Simple calculations show that the state-space representation of $G_1(s)G_2(s)G_3(s)$ is

$$\mathbf{A}_{13} = \begin{bmatrix} \mathbf{A}_1 & \mathbf{0} & \mathbf{0} \\ \mathbf{B}_2\mathbf{C}_1 & \mathbf{A}_2 & \mathbf{0} \\ \mathbf{B}_3\mathbf{D}_2\mathbf{C}_1 & \mathbf{B}_3\mathbf{C}_2 & \mathbf{A}_3 \end{bmatrix} \tag{26}$$
$$\mathbf{B}_{13} = \begin{bmatrix} \mathbf{B}_1 \\ \mathbf{B}_2\mathbf{D}_1 \\ \mathbf{B}_3\mathbf{D}_2\mathbf{D}_1 \end{bmatrix} \tag{27}$$
$$\mathbf{C}_{13} = [\mathbf{D}_2\mathbf{D}_2\mathbf{C}_1 \;\; \mathbf{D}_3\mathbf{C}_2 \;\; \mathbf{C}_3] \tag{28}$$
$$\mathbf{D}_{13} = \mathbf{D}_3\mathbf{D}_2\mathbf{D}_1 \tag{29}$$

Only $G_2(s)$ is being reset. Since $\mathbf{D}_1 = \mathbf{D}_2 = \mathbf{D}_3 = \mathbf{0}$, it is also straightforward to show that

$$\dot{\mathbf{x}}_{13} = \mathbf{A}\mathbf{x}_{13} + \mathbf{B}u_1, \quad \text{if } u_1 \neq 0 \tag{30}$$
$$\mathbf{x}_{13}^+ = \mathbf{A}_{\rho,13}\mathbf{x}_{13}, \quad \text{if } u_1 = 0 \tag{31}$$
$$y_3 = \mathbf{C}\mathbf{x}_3 \tag{32}$$
$$\mathbf{A}_{13} = \begin{bmatrix} \mathbf{A}_1 & \mathbf{0} & \mathbf{0} \\ \mathbf{B}_2\mathbf{C}_1 & \mathbf{A}_2 & \mathbf{0} \\ \mathbf{0} & \mathbf{B}_3\mathbf{C}_2 & \mathbf{A}_3 \end{bmatrix} \tag{33}$$
$$\mathbf{B}_{13} = \begin{bmatrix} \mathbf{B}_1 \\ \mathbf{0} \\ \mathbf{0} \end{bmatrix} \tag{34}$$
$$\mathbf{C}_{13} = [\mathbf{0} \;\; \mathbf{0} \;\; \mathbf{C}_3] \tag{35}$$
$$\mathbf{A}_{\rho,13} = \begin{bmatrix} \mathbf{I} & \mathbf{0} & \mathbf{0} \\ \mathbf{0} & \gamma & \mathbf{0} \\ \mathbf{0} & \mathbf{0} & \mathbf{I} \end{bmatrix} \tag{36}$$

3.2 Performance in simulation

This modification achieves the same describing function of the Clegg integrator with lower higher harmonics, i.e. for the same sinusoidal input its output is closer to a sinusoid than the output of the Clegg integrator all alone. An example is shown in Figure 3 for a Clegg integrator with a phase of 79.7° and a modified Clegg integrator consisting in three blocks in series as in Figure 2 set to achieve the same phase. The fractional derivatives of the modified Clegg integrator were implemented using a CRONE approximation and will thus only behave as expected in the frequency range $[\omega_l, \omega_h]$ where its zeros and poles are interlaced. Notice how the harmonics are clearly smaller with the fractional derivatives. The gain is not relevant for the comparison, since it behaves linearly and can thus be raised or lowered by varying the controller's gain.

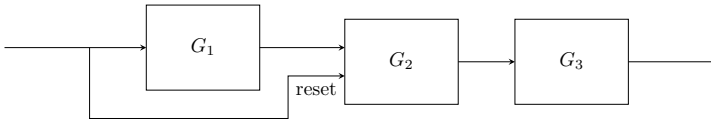

Fig. 2. Block diagram of three systems in series.

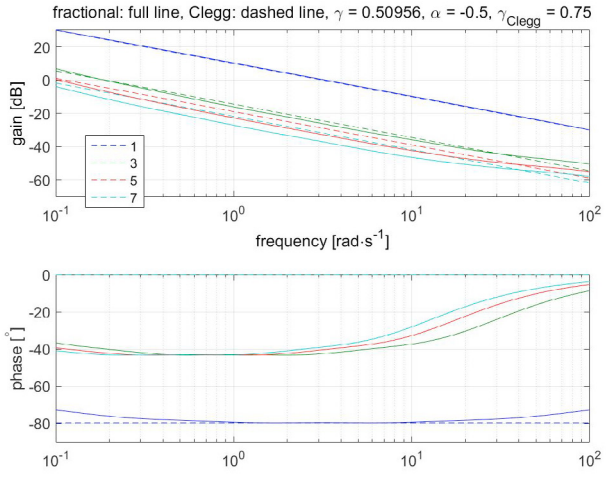

Fig. 3. Dashed line: describing function of a Clegg integrator; the reset coefficient is $\gamma = 0.75$; harmonics 1, 3, 5 and 7 (even numbered ones are zero) are shown. Full line: describing function of a modified Clegg consisting of three block in series; the reset coefficient is $\gamma = 0.51$; the fractional order is $\alpha = 0.5$; CRONE approximations in frequency range $[\omega_l, \omega_h] = [0.01, 100]$ rad/s with $N = 4$ zeros and poles were used.

4. FIRST ORDER RESET ELEMENT (FORE)

A first order reset system (FORE) is based on a first order system. It is given by (Horowitz and Rosenbaum, 1975)

$$\dot{\mathbf{x}} = -\omega_c \mathbf{x} + \omega_c u, \qquad \text{if } u \neq 0 \tag{37}$$

$$\mathbf{x}^+ = \mathbf{A}_\rho \mathbf{x}, \qquad \text{if } u = 0 \tag{38}$$

$$y = \mathbf{x} \tag{39}$$

Without reset ($\mathbf{A}_\rho = \mathbf{0}$), a linear first order system is obtained. Notice that the reset matrix $\mathbf{A}_\rho$ is in fact scalar.

The gain of a FORE's describing function is similar to the gain of a first order system's frequency response. However, its phase is closer to zero. This is illustrated in Figure 4. The block diagram in Figure 5 represents a FORE. The FORE can be generalised to second order reset element (SORE) (Hazeleger et al., 2016) or to a reset fractional order controller (Chen et al., 2020). Neither will be addressed in this paper.

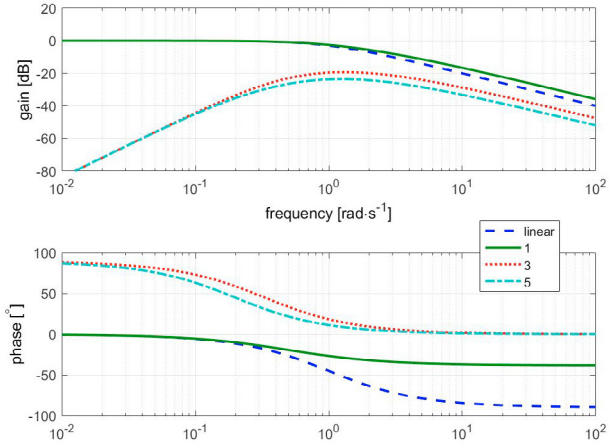

Fig. 4. Dashed line: frequency response of a first order filter with $\omega_c = 1$ rad/s. Full line, dotted line, dash-dotted line: describing function of the corresponding FORE (harmonics 1, 3 and 5).

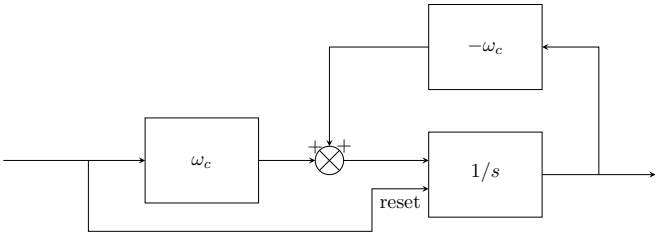

Fig. 5. Block diagram of a FORE.

4.1 FORE of three blocks in series (FORE3s)

Suppose that, in Figure 5, the integration $\frac{1}{s}$ is replaced by three blocks in series as in Figure 2. The resulting modified FORE is shown in Figure 6. The state equations will have a reset matrix $\mathbf{A}'_\rho$ with only one non-zero element in the diagonal, that will reset the state of $G_2(s)$. This FORE of three blocks in series will henceforth be abbreviated as FORE3s.

We already know that the state-space representation of the three systems in series is given by (26)–(29). Since $\mathbf{D}_1 = \mathbf{D}_2 = \mathbf{D}_3 = \mathbf{0}$, it is straightforward to show that, for the FORE feedback loop,

$$\begin{aligned}\dot{\mathbf{x}}_{13} &= \mathbf{A}_{13}\mathbf{x}_{13} + \mathbf{B}_{13}\omega_c(u - y_3) \\ &= \mathbf{A}_{13}\mathbf{x}_{13} + \omega_c\mathbf{B}_{13}u - \omega_c\mathbf{B}_{13}\mathbf{C}_{13}\mathbf{x}_{13} \\ &= (\mathbf{A}_{13} - \omega_c\mathbf{B}_{13}\mathbf{C}_{13})\,\mathbf{x}_{13} + \omega_c\mathbf{B}_{13}u, \quad \text{if } u \neq 0\end{aligned} \tag{40}$$

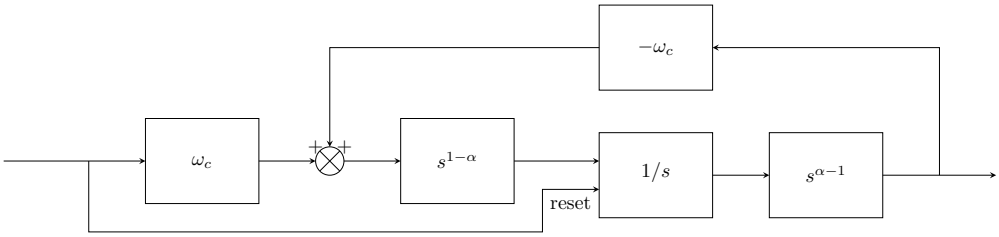

Fig. 6. Block diagram of a FORE3s controller.

From here, the state-space representation of a FORE3s is found as

$$\dot{\mathbf{x}}_{13} = \mathbf{A}\mathbf{x}_{13} + \mathbf{B}u_1, \qquad \text{if } u_1 \neq 0 \tag{41}$$
$$\mathbf{x}_{13}^{+} = \mathbf{A}_{\rho,13}\mathbf{x}_{13}, \qquad \text{if } u_1 = 0 \tag{42}$$
$$y_3 = \mathbf{C}\mathbf{x}_3 \tag{43}$$
$$\mathbf{A} = \begin{bmatrix} \mathbf{A}_1 & \mathbf{0} & -\omega_c\mathbf{B}_1\mathbf{C}_3 \\ \mathbf{B}_2\mathbf{C}_1 & \mathbf{A}_2 & \mathbf{0} \\ \mathbf{0} & \mathbf{B}_3\mathbf{C}_2 & \mathbf{A}_3 \end{bmatrix} \tag{44}$$
$$\mathbf{B} = \begin{bmatrix} \omega_c\mathbf{B}_1 \\ \mathbf{0} \\ \mathbf{0} \end{bmatrix} \tag{45}$$
$$\mathbf{C} = [\mathbf{0}\ \mathbf{0}\ \mathbf{C}_3] \tag{46}$$
$$\mathbf{D} = \mathbf{0} \tag{47}$$
$$\mathbf{A}_{\rho,13} = \begin{bmatrix} \mathbf{I} & \mathbf{0} & \mathbf{0} \\ \mathbf{0} & \mathbf{A}'_\rho & \mathbf{0} \\ \mathbf{0} & \mathbf{0} & \mathbf{I} \end{bmatrix} \tag{48}$$

4.2 Three blocks in series, the second is a FORE (3sFORE)

However, a different arrangement of blocks is possible. Rather than a FORE of three blocks in series, it is possible to use a FORE as the second element of three blocks in series, i.e. make

$$G_1(s) = s^{1-\alpha} \tag{49}$$
$$G_3(s) = s^{\alpha-1} \tag{50}$$

in Figure 2, and let $G_2(s)$ be a FORE as shown in Figure 5. Again, reset is done considering the input of the first block. The new reset matrix $\mathbf{A}'_\rho$ will be scalar. This combination of "three blocks in series, the second is a FORE" will henceforth be abbreviated as 3sFORE. It is shown in Figure 7.

It is necessary to optimise the reset coefficient $\mathbf{A}'_\rho$ and the differentiation order α so that the behaviour of this modified FORE will be optimised. In what follows, the Nelder-Mead simplex search method, implemented in Matlab with `fminsearch`, was used like this: given a FORE with reset matrix $\mathbf{A}_\rho$, the Nelder-Mead simplex search sought values of $\mathbf{A}'_\rho$ and α such that the lowest value of the phase of $G_1(s)G_2(s)G_3(s)$ should be the same as the phase of a Clegg integrator with reset coefficient $\mathbf{A}_\rho$.

Let us denote the state space matrixes of $G_1(s)$, given by a CRONE approximation of (23), as $\mathbf{A}_1$, $\mathbf{B}_1$, $\mathbf{C}_1$ and $\mathbf{D}_1$. Let us denote the state space matrixes of FORE $G_2(s)$, given by (37)–(39), as $\mathbf{A}_2$, $\mathbf{B}_2$, $\mathbf{C}_2$ and $\mathbf{D}_2$. Let us denote the state space matrixes of $G_3(s)$, given by a CRONE approximation of (25), as $\mathbf{A}_3$, $\mathbf{B}_3$, $\mathbf{C}_3$ and $\mathbf{D}_3$. Then the state-space representation of a 3sFORE is

$$\dot{\mathbf{x}}_{13} = \mathbf{A}_{13}\mathbf{x}_{13} + \mathbf{B}_{13}u_1, \qquad \text{if } u_1 \neq 0 \tag{51}$$
$$\mathbf{x}_{13}^{+} = \mathbf{A}_{\rho,13}\mathbf{x}_{13}, \qquad \text{if } u_1 = 0 \tag{52}$$
$$y_3 = \mathbf{C}_{13}\mathbf{x}_3 + \mathbf{D}_{13}u_1 \tag{53}$$
$$\mathbf{A}_{12} = \begin{bmatrix} \mathbf{A}_1 & \mathbf{0} \\ \mathbf{B}_2\mathbf{C}_1 & \mathbf{A}_2 \end{bmatrix} \tag{54}$$
$$\mathbf{B}_{12} = \begin{bmatrix} \mathbf{B}_1 \\ \mathbf{B}_2\mathbf{D}_1 \end{bmatrix} \tag{55}$$
$$\mathbf{C}_{12} = [\mathbf{D}_2\mathbf{C}_1\ \mathbf{C}_2] \tag{56}$$
$$\mathbf{D}_{12} = \mathbf{D}_2\mathbf{D}_1 \tag{57}$$
$$\mathbf{A}_{13} = \begin{bmatrix} \mathbf{A}_{12} & \mathbf{0} \\ \mathbf{B}_3\mathbf{C}_{12} & \mathbf{A}_3 \end{bmatrix} \tag{58}$$
$$\mathbf{B}_{13} = \begin{bmatrix} \mathbf{B}_{12} \\ \mathbf{B}_3\mathbf{D}_{12} \end{bmatrix} \tag{59}$$
$$\mathbf{C}_{13} = [\mathbf{D}_3\mathbf{C}_{12}\ \mathbf{C}_3] \tag{60}$$
$$\mathbf{D}_{13} = \mathbf{D}_3\mathbf{D}_{12} \tag{61}$$
$$\mathbf{A}_{\rho,13} = \begin{bmatrix} \mathbf{I} & \mathbf{0} & \mathbf{0} \\ \mathbf{0} & \mathbf{A}'_\rho & \mathbf{0} \\ \mathbf{0} & \mathbf{0} & \mathbf{I} \end{bmatrix} \tag{62}$$

5. CONSTANT IN GAIN LEAD IN PHASE CONTROLLER (CGLP)

A CgLp, shown in Figure 8, consists in a FORE followed by a (linear) lead compensator (Saikumar et al., 2019) with the same cutoff frequencies. The FORE has a gain that decreases with frequency, while the lead compensator has a gain that increases with frequency. The net result is a gain which is constant with frequency (or at least close to constant, since around the cutoff frequency the evolution of both gains is not symmetrical). The phase of the lead compensator goes up to 90°, while the phase of the FORE goes down to a value which is not as low as −90°. The net result is a phase that increases with frequency. This behaviour can be seen in Figure 9 and in Figure 10.

The CgLp is used to improve (i.e. increase) the phase margin, without changing the gain. If only a lead compensator were used, the phase would also go up, but the increase of gain with frequency would increase the gain crossover frequency, and thus the improvement in the phase margin would be smaller or even non-existent. Just as a FORE can be generalised to a SORE, a CgLp can also be built with a SORE and a second order linear filter (Saikumar et al., 2019); it can also be improved with a shaping filter to become a band-passed CgLp, with the nonlinearity suppressed in a desired frequency range (Karbasizadeh et al., 2023). Neither will be addressed in this paper.

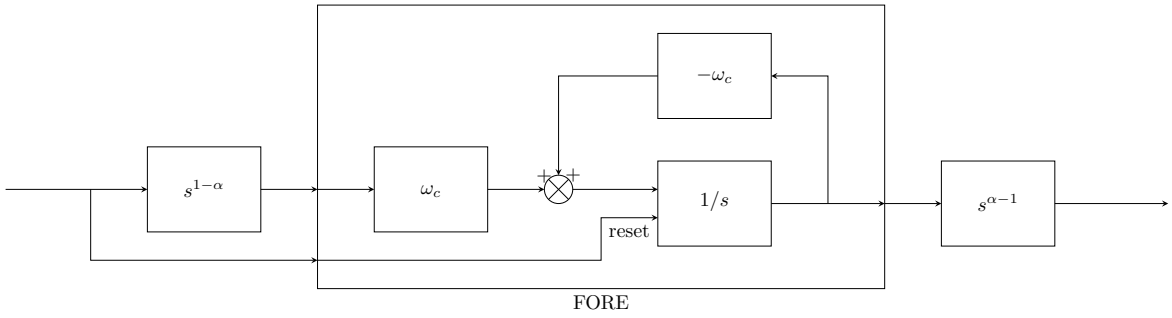

Fig. 7. Block diagram of a 3sFORE controller.

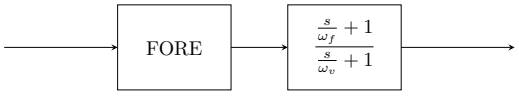

Fig. 8. Block diagram of a CgLp.

5.1 Modified CgLp: 3sCgLp and CgLp3s

A CgLp can be built using a 3sFORE or a FORE3s. Just as these variations of a FORE have an improved performance, that of the CgLp will improve too. The configuration in which Figure 7 is used in Figure 8 will henceforth be called a 3sCgLp, and that in which Figure 6 is used in Figure 8 will be called a CgLp3s.

5.2 Performance in simulation

Figure 9 shows results for a 3sCgLp; Figure 10 shows results for a CgLp3s. In both, higher order harmonics are lower than with a CgLp. This happens even though the reset coefficient γ is lower, and thus the system more non-linear. For good results, the CRONE approximation should use a frequency range $[\omega_l, \omega_h]$ below the cutoff frequency of the FORE ω_c. This will decrease higher order harmonics up to ω_c, which is where this decrease is probably more important, without deteriorating the behaviour above ω_c.

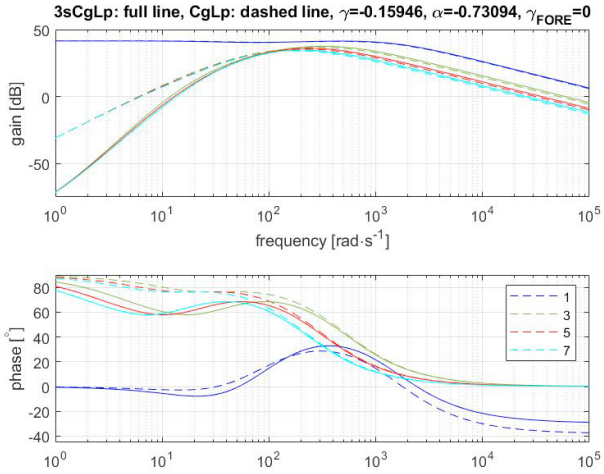

Fig. 9. Full lines: describing function of a 3sCgLp for $\omega_c = 150$ Hz, $\omega_f = \omega_c/1.97$ and $\omega_v = 10\omega_c$; a CRONE approximation with $N = 2$ zeros and poles in frequency range $[\omega_l, \omega_h] = [10, 100]$ Hz was used for fractional derivatives. Harmonics 1, 3, 5 and 7 are shown and compared with those of a CgLp (dashed lines, same colours for the same harmonics).

6. CONCLUSION

Employing reset control with fractional derivatives lowers higher order harmonics resulting from the non-linearity of reset. This has been shown in this paper with several examples, using numerical optimisation to find the fractional order α and the reset matrix $\mathbf{A}_\rho$.

The reason why this happens is because all the configurations studied have, in one way or another, three systems in series; furthermore, the *second* system is reset according to the input of the *first*, i.e. of system G_1, which is a lead element. Consequently, the reset of G_2 happens when it is closer to 0°; in other words, the discontinuity due to reset is less marked. It is for this reason that higher order harmonics are lower. Instead of fractional derivatives, other lead elements could be used for G_1, provided that G_3 would be a corresponding lag element. But fractional derivatives are a simple choice and are easy to tune. Of course, the fractional derivative must be approximated accurately in the frequency range where it must act as lead.

As future work, a PID based upon a CgLp should be studied in a similar manner. Applications to mechatronic systems, such as in (HosseinNia et al., 2013), can be envisaged. The robustness of these controllers with reset must be compared with that of the original linear ones. The expected reduction in each harmonic could eventually be computed, rather than left to the result of the numerical optimisation.

REFERENCES

Chen, L., Saikumar, N., and HosseinNia, S.H. (2020). Development of robust fractional-order reset control. *IEEE Transactions on Control Systems Technology*, 28(4), 1404–1417. Http://doi.org/10.1109/TCST.2019.2913534.

Clegg, J.C. (1958). A nonlinear integrator for servomechanisms. *Transactions of the American Institute of Electrical Engineers, Part II: Applications and Industry*, 77(1), 41–42.

Guo, Y., Wang, Y., and Xie, L. (2009). Frequency-domain properties of reset systems with application in hard-disk-drive systems. *IEEE Transactions on Control Systems Technology*, 17(6), 1446–1453.

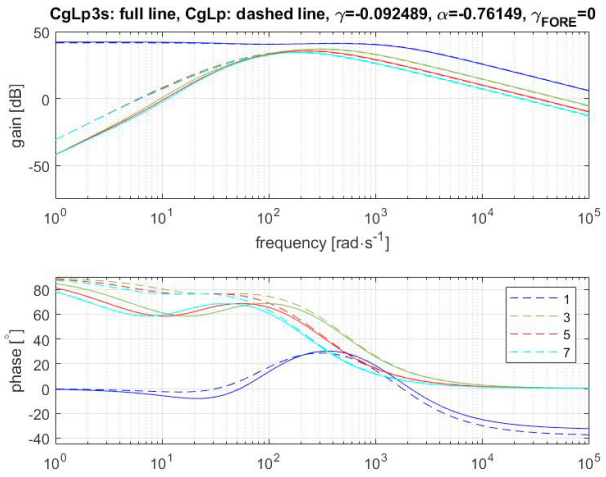

Fig. 10. Full lines: describing function of a CgLp3s for $\omega_c = 150$ Hz, $\omega_f = \omega_c/1.97$ and $\omega_v = 10\omega_c$; ; a CRONE approximation with $N = 2$ zeros and poles in frequency range $[\omega_l, \omega_h] = [10, 100]$ Hz was used for fractional derivatives. Harmonics 1, 3, 5 and 7 are shown and compared with those of a CgLp (dashed lines, same colours for the same harmonics).

Hazeleger, L., Heertjes, M., and Nijmeijer, H. (2016). Second-order reset elements for stage control design. In *American Control Conference*.

Horowitz, I. and Rosenbaum, P. (1975). Non-linear design for cost of feedback reduction in systems with large parameter uncertainty. *International Journal of Control*, 21(6), 977–1001.

HosseinNia, S.H., Tejado, I., and Vinagre, B.M. (2013). Fractional-order reset control: Application to a servo-motor. *Mechatronics*, 23(7), 781–788.

Karbasizadeh, N., Dastjerdi, A.A., Saikumar, N., and HosseinNia, S.H. (2023). Band-passing nonlinearity in reset elements. *IEEE Transations on Control Systems Technology*, 31(1), 333–343.

Karbasizadeh, N., Saikumar, N., and HosseinNia, S.H. (2021). Fractional-order single state reset element. *Nonlinear Dynamics*, 104, 413–427.

Nuij, P.W.J.M., Bosgra, O.H., and Steinbuch, M. (2006). Higher-order sinusoidal input describing functions for the analysis of non-linear systems with harmonic responses. *Mechanical Systems and Signal Processing*, 20, 1883–1904.

Saikumar, N., Heinen, K., and HosseinNia, S.H. (2021). Loop-shaping for reset control systems: A higher-order sinusoidal-input describing functions approach. *Control Engineering Practice*, 111, 104808.

Saikumar, N., Heinen, K., and HosseinNia, S.H. (2023). Corrigendum to "Loop-shaping for reset control systems: A higher-order sinusoidal-input describing functions approach" [Control Engineering Practice 111 (2021) 104808]. *Control Engineering Practice*, 137, 105565.

Saikumar, N. and HosseinNia, H. (2017). Generalized fractional order reset element (GFrORE). In *9th European Nonlinear Dynamics Conference (ENOC)*.

Saikumar, N., Sinha, R.K., and HosseinNia, S.H. (2019). 'Constant in gain lead in phase' element — application in precision motion control. *IEEE/ASME Transactions on Mechatronics*. Http://doi.org/10.1109/TMECH.2019.2909082.

Yang, X., Peng, D., and Xiaoxiao Lv, X.L. (2019). Recent progress in impulsive control systems. *Mathematics and Computers in Simulation*, 155, 244–268.